TRIBOLOGY TRANSACTIONS
2019, VOL. 62, NO. 6, 1129–1141
https://doi.org/10.1080/10402004.2019.1654052

Life Model Enhancement for Hybrid Ball Bearings

Pradeep K. Gupta[a] and Erwin V. Zaretsky[b]

[a]PKG Inc., Clifton Park, NY, USA; [b]Erwin V. Zaretsky, PE, Chagrin Falls, OH, USA

ABSTRACT

Based on experimental life data on silicon nitride balls, the stress-life exponent and life constant in the generalized ball life equation, developed earlier, are modified to better simulate the fatigue life of silicon nitride balls in hybrid ball bearings. The modified ball life equation is then integrated with generalized life equations for the outer and inner races to model the life of a complete hybrid ball bearing. It is found that in view of the relatively high stress-life exponent for silicon nitride balls, computation of hybrid bearing life with infinite ball life may not be unreasonable. Model predictions are in good agreement with limited available experimental life data on hybrid ball bearings.

ARTICLE HISTORY
Received 5 March 2019
Accepted 3 August 2019

KEYWORDS
Fatigue life; hybrid ball bearings; rolling contact fatigue; rolling bearings; ADORE

Introduction

It is well established that the higher modulus of elasticity of silicon nitride, under prescribed geometry and applied load, leads to higher contact stress between a steel race and a silicon nitride ball, in comparison to that obtained with an all-steel contact. Though the difference in contact life of silicon nitride and steel rolling elements at any stress is subject to the differences in fatigue behavior of the two materials, the contact lives of the steel races are definitely reduced with the increased contact stress in hybrid contacts. Such a reduction in the life of bearing races has led to a common speculation that under a prescribed applied load, the life of a hybrid bearing is less than that obtained with an all-steel bearing. Although for most relatively low-speed applications such a speculation may be valid, in general, the contact loads at the rolling element–to-race contacts in a rolling bearing under a prescribed applied load and speed may not be the same between the all-steel and hybrid bearings even when the race and rolling element geometries are identical. For example, in an angular contact ball bearing, the reduced centrifugal forces and increased contact stiffness with silicon nitride balls result in altered contact angles, which lead to a change in contact loads. Likewise, in radially loaded cylindrical roller bearings, the increased stiffness with silicon nitride rollers alters the load distribution in the bearing, which affects the contact loads; in addition, the reduced centrifugal forces on silicon nitride rollers alter the contact loads.

In addition to the above geometrical effects, the stress-life exponent and base life constant in the silicon nitride rolling element life equation may be different from those for the steel rolling element. This impacts the rolling element life under any stress, which in turn affects the overall bearing life. Therefore, in lieu of simple replacement of steel rolling elements with silicon nitride elements of identical geometry, a thorough redesign of the internal geometry of a hybrid bearing to optimize the contact stresses and resulting life is necessary. Though the geometrical effects are modeled by load–deflection analysis for the bearing, enhancement of the life equation for silicon nitride balls for improved design and performance simulation of hybrid ball bearings is the primary objective of this investigation.

The majority of rolling bearing life estimates in practical bearing designs have been based on the original Lundberg-Palmgren (LP) model (Lundberg and Palmgren *(1, 2)*). This formulation is based on unpublished experimental fatigue life data for a large number of bearings made with the pre-1950 AISI 52100 bearing steel. The model is based on Weibull's *(3)* fatigue hypothesis, which relates the fatigue life to an integral of a subsurface stress function over the stressed volume. By relating the subsurface critical failure stress and stressed volume to the bearing geometry, the LP life equation (Lundberg and Palmgren *(1, 2)*) expresses life simply in terms of geometrical parameters of the bearing, and properties of the AISI 52100 steel are part of the empirical constant; in addition, the shear stress exponent in the stress function is included as part of other exponents in the life equation. In addition, bearing life is segmented into outer and inner race lives only, with no provision for an independent treatment of rolling element life. Because the model constant is developed by correlating the bearing life prediction with that obtained experimentally, the life of rolling elements is implicit in the computed race lives.

CONTACT Pradeep K. Gupta guptap@pradeepkguptainc.com
Color versions of one or more of the figures in the article can be found online at www.tandfonline.com/utrb.
Review led by N. Weinzapfel.
Pradeep K. Gupta is an STLE Fellow.
Erwin V. Zaretsky is an STLE Fellow.

Nomenclature

A_{GZ}	Empirical constant in GZ dynamic stress capacity equation. Units depend on exponent c; = Default value for all steel bearings = 6.4229×10^8 N/m$^{1.777}$
A_{LP}	Empirical constant in LP dynamic stress capacity equation. Units depend on exponents c and h; = Default value for all steel bearings = 1.4599×10^9 N/m$^{1.933}$
a	Major contact half width (m)
a^*	Dimensionless major contact half width for point contact
b	Minor contact half width (m)
b^*	Dimensionless minor contact half width for point contact
c	Shear stress-life exponent. Default value = 31/3
D	Rolling element diameter (m)
E	Modulus of elasticity (Pa)
E'	Effective elastic modulus parameter for contact surfaces (Pa)
G	Geometric parameter in dynamic stress capacity equation. Units depend on exponents c and h
h	Subsurface shear stress depth exponent. Default value = 7/3
L	Fatigue life (h)
m	Weibull modulus or slope
p_H	Applied Hertzian contact stress (Pa)
p_{Hc}	Dynamic stress capacity (Pa)
u	Number of stress cycles of revolution of rotating race
ζ	Ratio of critical failure stress to maximum Hertzian contact stress
η	Ratio of effective contact width to major contact half width
$\dot{\theta}$	Rolling element orbital velocity (rad/s)
κ	Model constant
λ_E	Material parameter (ratio of E' to E'_{52100})
υ	Poisson's ratio
ξ	Ratio of depth of critical failure stress to contact minor half width
$\sum\rho$	Curvature sum of contacting surfaces (1/m)
τ_o	Maximum orthogonal shear stress (Pa)
τ_m	Maximum shear stress (Pa)
Φ	Dynamic stress capacity adjustment factor
Ω	Race angular velocity (rad/s)
ω_b	Rolling element angular velocity (rad/s)

Subscripts

GZ	Gupta-Zaretsky model
LP	Lundberg-Palmgren model
10	10% failure probability (90% survival probability)

When the life equation only contains geometrical variables, modeling of bearing materials other than AISI 52100 bearing steel becomes difficult with this original form of the life equation. Most implementations of the LP life equations to hybrid bearings only adjust the contact stress to reflect a steel versus silicon nitride contact. An example is the work by Zaretsky *(4)*, where the LP equation, with modified contact stress, is used to compute the life of a 57-mm cylindrical hybrid roller bearing. Although the computed results showed reasonable correlation with experimental life data published by Baumgartner and Cowley *(5)* and Baumgartner, et al *(6)*, examination of failed bearings revealed unusual number of roller failures with significant roller damage, including fracture.

In order to more effectively implement the LP life model to rolling bearings with arbitrary bearing materials, Gupta and Zaretsky *(7)* have recently presented a generalized form of the LP equation in terms of distinct material and geometrical parameters, and the empirical constant, which is estimated by correlation of model predictions with experimental bearing life data, is independent of material properties. In addition, independent life equations for the races and rolling elements are presented, where the empirical exponents and constants may be arbitrarily modified to better model the behavior of the race and rolling element materials. Of course, when both the race and rolling element materials are set to AISI 52100, the life predictions obtained with the generalized formulation reduce to those obtained with the original LP equation.

In addition to generalization of the LP life equation, Gupta and Zaretsky *(7)* have introduced a new life model based on earlier work of Zaretsky *(8)*. This newly introduced model makes three fundamental modifications to the LP equation: first explicit life dependence on subsurface depth of the failure stress is eliminated; secondly, the maximum subsurface orthogonal shear stress used by Lundberg and Palmgren is replaced by the maximum subsurface shear stress; and, finally, data variability in the stress-life exponent is eliminated. With these modifications, the new Gupta-Zaretsky (GZ) model better conforms to the original Weibull postulation (Weibull *(3)*). The first two of these modifications have also been implemented by Yu and Harris *(9)*, who presented a generalized life model for a ball bearing in terms of a numerically rigorous integration of the stress function over the stressed volume, similar to the one developed by Ioannides and Harris *(10)*. However, the empirical constant in the life equation is still estimated by correlation of model prediction against experimental bearing life data. Gupta and Zaretsky *(7)* have demonstrated that when the empirical model constant is estimated by correlation of model prediction with the experimental life data, a numerically intensive integration of the stress function over the stressed volume does not provide any greater precision in life prediction over the simple product of constant stress function and the applicable stressed volume, as used by Lundberg and Palmgren *(1, 2)*.

Because life models for both ball and roller bearings are based on the fundamental Weibull hypothesis (Weibull *(3)*), the empirical constants in the dynamic stress capacity equations for ball and roller bearings may be related to the fundamental proportionality constant in the Weibull hypothesis, as suggested by Gupta and Zaretsky *(7)*. Thus, unlike the original LP formulation, where the empirical constants in dynamic load capacity equations for ball and roller bearings are independently determined, the applicable constant for roller bearings in the newly developed generalized life equation may be readily derived from the one estimated for ball bearings. In view of these generalities and relatively easy implementation, the generalized life equations (Gupta and Zaretsky *(7)*) provide a viable starting point for the present

investigation, where the objective is to enhance the life equation for the silicon nitride ball in a hybrid ball bearing.

The experimental data on the fatigue behavior of silicon nitride balls generated by Parker and Zaretsky *(11)* are perhaps the only available experimental data suitable for the development of independent life equation for a silicon nitride ball in a hybrid ball bearing. This work used a unique five-ball tester to generate rolling contact fatigue failure data on a silicon nitride ball in contact with four AISI M50 steel balls. For comparison purposes, the tester was also used to generate life data for AISI 52100 and AISI M50 balls (Parker and Zaretsky *(12, 13)*). These experimental data provide a baseline for the enhancements of shear stress exponent and empirical constant in the silicon nitride ball life equation in the present investigation.

Once an independent life equation for the silicon nitride ball is established, life prediction of a hybrid ball bearing still requires validation against experimental fatigue life data obtained with full-scale hybrid bearings. Unfortunately, such experimental investigations are still in the development stages. The very recent data presented by Trivedi, et al. *(14)* only provide a starting point. Therefore, in the present investigation these data only provide an initial validation of model predictions. As additional life data on hybrid bearings become available, continued updates of model constants and stress-life exponents may be necessary. Such updates are readily facilitated in the generalized models presented in this article.

Rolling element life model enhancement

Both the generalized LP and the newly introduced GZ models, as presented by Gupta and Zaretsky *(7)*, permit independent variations in the geometrical and material parameters for the races and rolling elements. Whereas the geometrical parameters permit a change in the operating geometry of bearing elements as a function of operating speed and temperature, the material parameters permit arbitrary selection of materials and facilitate modeling of property variation as a function of operating temperature for each of the bearing elements. Thus, these generalized models provide a technically sound baseline for the development of life equations for silicon balls in hybrid bearings.

Symbolically, for a point contact configuration in ball bearings, the generalized equations for ball life at each ball-to-race contact in a ball bearing are summarized below.

LP Model: The generalized LP stress-life relationship is summarized as

$$L_{LP} = \left(\frac{p_{HcLP}}{p_H}\right)^{\frac{c+2-h}{m}} \quad [1a]$$

$$p_{H_{cLP}} = \Phi_{LP} A_{LP} \kappa_{LP}^{-\frac{1}{c+2-h}} \lambda_E^{\frac{2-h}{c+2-h}} G_{LP}^{-\frac{1}{c+2-h}} u^{-\frac{m}{c+2-h}} \quad [1b]$$

$$\text{Constant, } \kappa_{LP} = \frac{\eta \zeta_{LP}^{c} \xi_{LP}^{1-h}}{a_1} \quad [1c]$$

$$\text{Reliability factor, } a_1 = \frac{\ln \frac{1}{S}}{\ln \frac{1}{0.90}} \quad [1d]$$

$$\text{Shear stress ratio, } \zeta_{LP} = \frac{\tau_o}{p_H} = 0.25(\text{default}) \quad [1e]$$

$$\text{Shear stress depth ratio, } \xi_{LP} = \frac{z_o}{b} = 0.50(\text{default}) \quad [1f]$$

$$\text{Contact width ratio, } \eta = \frac{\text{contact width}}{a} = 2(\text{default}) \quad [1g]$$

$$\text{Material parameter, } \lambda_E = \frac{E'}{E'_{52100}} \quad [1h]$$

$$\text{Geometrical parameter, } G_{LP} = D\left(\frac{1}{\sum \rho}\right)^{2-h} a^{*3-h} b^{*3-2h} \quad [1i]$$

$$\text{Cycling frequency, } u = \left|\frac{\omega_b - \dot{\theta}}{\Omega_r}\right|. \quad [1j]$$

Here E' is the commonly used composite elastic properties parameter for the two interacting elastic solids, $1/E' = (1-\upsilon_1^2)/E_1 + (1-\upsilon_2^2)/E_2$. The factor Φ_{LP}, presently set to 1 (one), is for future use when the empirical constant is modified for further customization of the model. Lundberg-Palmgren *(1, 2)* have proposed values of 31/3, 7/3, and 10/9, respectively, for the exponents c, h, and m. These values have been effectively used in virtually all life modeling efforts and they are well established as acceptable values in all rolling contact fatigue life equations. Because the exponent c defines the primary stress function, it is perhaps the most dominant input in the life equation. Therefore, for modeling of ceramic materials, the applicable value of c is altered while h and m are assumed to stay at default values. An acceptable change in the empirical constant A_{LP} is then computed by fitting the model predictions to experimental ball life data.

GZ Model: Similar to the LP equation, the ball life equation in the newly introduced GZ model is expressed as

$$L_{GZ} = \left(\frac{p_{HcGZ}}{p_H}\right)^{\frac{cm+2}{m}} \quad [2a]$$

$$p_{H_{cGZ}} = \Phi_{GZ} A_{GZ} \kappa_{GZ}^{-\frac{1}{cm+2}} \lambda_E^{\frac{2}{cm+2}} G_{GZ}^{-\frac{1}{cm+2}} u^{-\frac{m}{cm+2}} \quad [2b]$$

$$\text{Constant, } \kappa_{GZ} = \frac{\eta \zeta_{GZ}^{cm} \xi_{GZ}}{a_1} \quad [2c]$$

$$\text{Shear stress ratio, } \zeta_{GZ} = \frac{\tau_m}{p_H} = 0.30 \text{ (default)} \quad [2d]$$

$$\text{Shear stress depth ratio, } \frac{z_m}{b} = \xi_{GZ} = 0.786 \text{ (default)} \quad [2e]$$

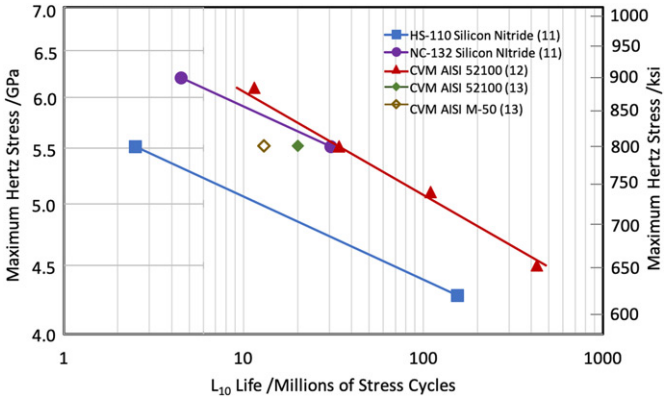

Figure 1. Experimental data on life of individual ball contacts, reproduced from the original data published by Parker and Zaretsky *(11)*.

$$\text{Geometrical parameter, } G_{GZ} = D\frac{(a^*b^*)^3}{(\sum \rho)^2}. \qquad [2f]$$

Again, the empirical constant A_{GZ} is determined by correlating model predictions to experimental life data. Similarly, the factor Φ_{GZ}, presently set to 1 (one), is for future customization of the empirical constant. The material parameter λ_E and the contact cycling frequency u are the same as those defined in Eqs. [1h] and [1j], respectively, for LP model.

In both the LP and GZ life models, the values of all exponents and empirical constant, as already established for all steel bearings (Gupta and Zaretsky *(7)*), are retained in the race life equations, and the applicable values in the ball life equations are modified in the present investigation to better fit the available experimental life data for silicon nitride balls.

Silicon nitride Hertz stress-life relation

Perhaps the only available experimental data on rolling contact fatigue of silicon nitride balls are due to Parker and Zaretsky *(11)*, who used the National Aeronautics and Space Administration's five-ball fatigue tester to investigate the fatigue life of silicon nitride balls as a function of contact stress. The observed lives are compared with those obtained earlier with other materials. The results are redrawn from the original data in Fig. 1.

Figure 1 presents silicon nitride ball life data for the hot-pressed HS-110 and NC-132 materials. These are early 1970s vintage materials. The HS-110 silicon nitride balls are from a billet of an earlier grade of hot-pressed silicon nitride material and the NC-132 is a later grade of silicon nitride material that is denser and more homogeneous and has a higher flexural strength than the earlier material HS-110. Intuitively, the NC-132 silicon nitride material would be expected to have a longer fatigue life than the HS-110 material. Indeed, this is the case, as seen in Fig. 1. The NC-132 silicon nitride material is more representative of those silicon nitride materials used in rolling element bearings today. This material is therefore considered in the current life model enhancement effort. Life differences in the two values for the CVM AISI 52100 balls are related to the variance between material batches. The Parker and Zaretsky CVM AISI 52100 data (Parker and Zaretsky *(12)*) have a greater number of test points and better define the stress-life relationship. By comparing the CVM AISI 52100 and NC-132 data in Fig. 1, it is clear that the two sets of data have different stress-life slopes and the two lines intersect at a stress point of 5.516 GPa (800 ksi). Thus, the lives of AISI 52100 and NC-132 balls are equal at this stress. Further analytical evaluation of these data leads to the following two significant findings related to the fatigue lives of silicon nitride balls:

1. The LP Hertz stress-life exponent for a silicon nitride ball is 16.
2. At a contact stress of 5.516 GPa (800 ksi), the lives of silicon nitride and AISI 52100 balls are equal.

There is indeed a question about relating contact lives observed with circular ball-to-ball contacts to actual bearings with an elliptical or line contact in ball and roller bearings, respectively. The current subsurface fatigue life models are based on an integral of a critical stress function over the stressed volume, irrespective of the contact geometry. Thus, though the life results obtained with a circular contact may be applied to actual bearing with elliptical contacts, the model constants should truly be derived by first formulating a model with circular contacts. However, at the National Aeronautics and Space Administration from 1979 to 1984, a large number of five-ball test runs were correlated to full-scale bearing tests, including extensive testing with 120-mm bore angular contact ball bearings as used by Gupta and Zaretesky *(7)*. These results have shown good correlation with those obtained with the five-ball tester. It should also be noted that analytically, because the stress-life exponent and model constant are derived by correlating the actual bearing contact lives to the observed circular contact lives, most of the variations between the circular and elliptical contact are included in the computed regression coefficients. Therefore, application of experimental data shown in Fig. 1 for the development of life models for actual bearings is well justified.

The findings from the five-ball test results, as documented above, may be applied to derive the shear stress exponent, c, and the applicable model constant for silicon nitride balls. First, by equating the stress-life exponent in Eq. [1] to the observed stress-life exponent value of 16, the applicable shear stress exponent c may be computed by the relation

$$\frac{c+2-h}{m} = 16. \qquad [3]$$

Substitution of the default LP values of $h = 7/3$ and $m = 10/9$ in Eq. [3] yields a shear stress exponent $c = 18.11$ for the silicon nitride balls. This value of c may be used in Eq. [2] to compute the GZ value of the applicable stress-life exponent of 19.91 for the silicon nitride balls. Using the second of the above two experimental findings, the rolling contact fatigue lives of silicon nitride and AISI 52100 steel

Table 1. Dynamic stress capacity constants for hybrid ball bearings.

Base Weibull slope, $m = 1.111$		
Model constant	LP model	GZ model
Depth exponent for silicon nitride, h	2.3333	0
Stress-life exponent for silicon nitride	$\frac{c+2-h}{m} = 16$	$\frac{cm+2}{m} = 19.911$
Shear stress exponent for silicon nitride, c	18.111	18.111
Empirical constant, A, for silicon nitride	$A_{LP} = 1.4732 \times 10^9$ N/m$^{1.962}$	$A_{GZ} = 9.3047 \times 10^8$ N/m$^{1.864}$
Base depth exponent for steel, h	2.3333	0
Base shear stress exponent for steel, c	10.3333	10.3333
Base stress-life exponent for steel	$\frac{c+2-h}{m} = 9$	$\frac{cm+2}{m} = 12.133$
Base empirical constant, A, for steel	$A_{LP} = 1.4599 \times 10^9$ N/m$^{1.933}$	$A_{GZ} = 6.4229 \times 10^8$ N/m$^{1.777}$

Table 2. Forty-millimeter angular contact ball bearing geometry.

Bearing bore	40 mm	Pitch diameter	60.25 mm
Bearing outer diameter	80 mm	Contact angle	22°
Number of balls	11	Outer race curvature factor	0.53
Ball diameter	12.70 mm	Inner race curvature factor	0.53

balls are equated, at a maximum Hertzian contact stress of 5.516 GPa (800 ksi), to determine the empirical constant in stress capacity equation for the silicon nitride balls. This is done for both LP and GZ models. The computed results for silicon nitride balls, along with the defaults values for steel races, as developed by Gupta and Zaretsky *(7)*, are summarized in Table 1.

Although the present investigation is directed toward ball bearings, the relationship between point and line contact constants, as developed by Gupta and Zaretsky *(7)*, may be used to estimate the applicable line contact constant. Thus, lives of silicon nitride rollers in hybrid roller bearings may also be modeled.

For parametric evaluation of life of a hybrid ball bearing, the above ball life equations along with the base formulations for the races, as developed by Gupta and Zaretsky *(7)*, are implemented in the ADORE bearing dynamics computer code (Gupta *(15)*). The predicted hybrid bearing lives are then validated against the recent experimental data presented by Trivedi, et al. *(14)*. However, before presenting these validations, the predicted ball life is validated against the Parker and Zaretsky *(11)* silicon nitride ball life data, as presented in Fig. 1. For this purpose, the 40-mm bore angular contact ball bearing, also used by Trivedi, et al. *(14)* in their full-scale hybrid bearing tests, is considered as an example. The bearing geometry is documented in Table 2.

In complete conformance to the contact configuration in five-ball tester used by Parker and Zaretsky *(11)*, individual ball contact lives for the ball-to–inner race contact in the 40-mm bore angular contact ball bearing are computed both with the ball material set as AISI 52100 steel and silicon nitride; the race material is set as AISI 52100 steel in both cases. The LP and GZ lives of silicon nitride and AISI 52100 balls are then plotted as a ratio, as a function of the inner race contact stress. The results are shown in Fig. 2.

These results are in complete conformance to the findings of Parker and Zaretsky *(11)*, as documented in Fig. 1. Similar results are also obtained with AISI M-50 steel races and other bearing geometries and operating speeds. In each case, the results are closely coincident with those shown in Fig. 2. Therefore, these results should be applicable to all bearing geometries and race materials. Higher lives at lower

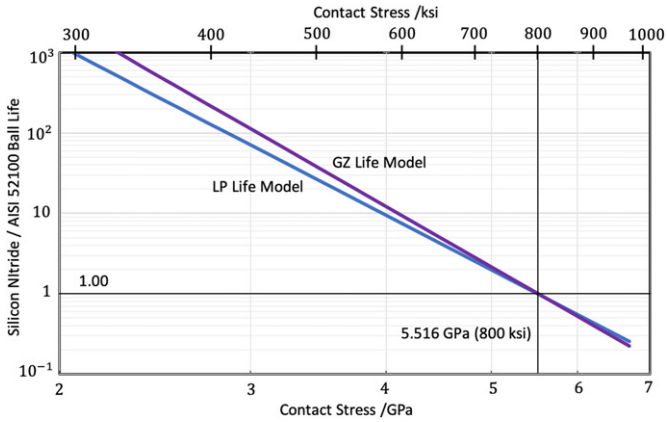

Figure 2. Silicon nitride ball life relative to the AISI 52100 ball life as a function of stress in the 40-mm hybrid ball bearing operating at room temperature (293 K) and at a shaft speed of 10,000 rpm.

stresses with the GZ model compared to the LP model are associated with the higher stress-life exponent in the GZ model.

Life modeling for complete hybrid bearing

Once the contact life of a silicon nitride ball is validated, as presented above, the enhanced bearing dynamics code, ADORE, is used to model life of a complete hybrid bearing. ADORE runs corresponding to the experimental hybrid bearing data for the 40-mm angular contact ball bearing, described in Table 2, are made and the model predictions are validated. As a starting point, two sets of parametric runs are made, the first one with VIMVAR AISI M-50 races and balls and the second one with VIMVAR AISI M-50 races and silicon nitride balls. For the all-steel bearing operating at 10,000 rpm, the lives of the ball, races, and complete bearing, as modeled by the generalized LP life model, are plotted in Fig. 3a as a function of inner race contact stress for the 40-mm ball bearing operating at 10,000 rpm. The figure includes the corresponding applied load axis so that the results may also be interpreted as a function of applied load. Because the bearing life is a statistical combination of the lives of the outer race, inner race, and balls, it is lower than the lowest of the individual bearing element lives.

Solutions corresponding to a hybrid bearing when the AISI M50 balls are replaced by silicon nitride balls are shown in Fig. 3b. A comparison of Figs. 3a and 3b reveals that at a given contact stress, the life of the hybrid bearing is higher than that of the all-steel bearing. This is primarily

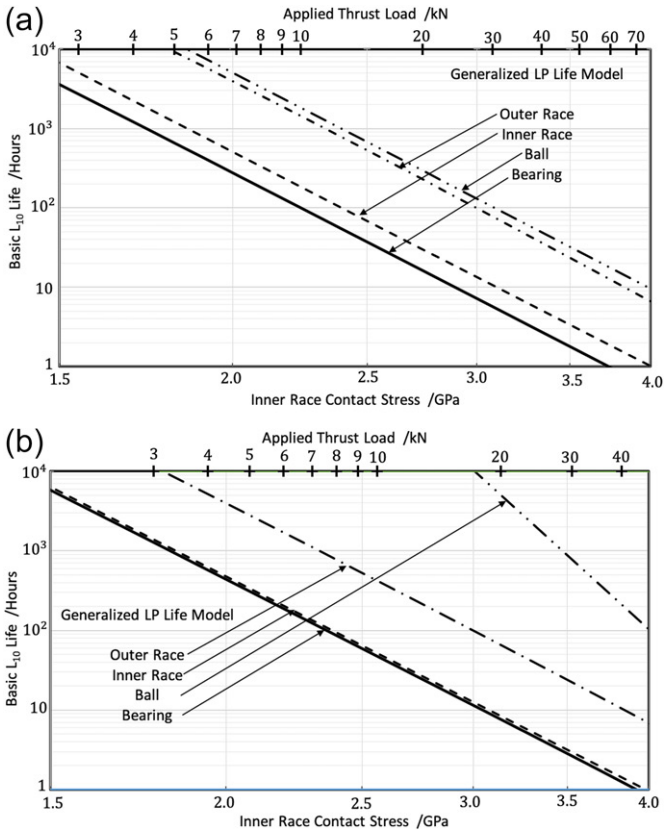

Figure 3. (a) Life distribution in the 40-mm bore VIMVAR AISI M-50 bearing at room temperature (293 K) and a shaft speed of 10,000 rpm, as predicted by the generalized LP model, (b) Life distribution in the 40-mm bore hybrid bearing with VIMVAR AISI M-50 races and silicon nitride balls, at room temperature (293 K) and a shaft speed of 10,000 rpm, as modeled by the generalized LP model.

due to the significantly higher life of silicon nitride balls at a given contact stress, resulting from the ball life enhancements presented above. The race lives, at a given contact stress, are almost identical between the steel and hybrid bearings in Figs. 3a and 3b. The slight reduction in race lives in the hybrid bearing is due to a small increase in the effective elastic modulus applicable at the hybrid ball–-race contacts.

Another notable observation in the hybrid bearing solution in Fig. 3b is that the bearing life is very close to the life of the inner race. This is due to the fact that the silicon nitride ball life is orders of magnitude greater than the race lives. In fact, the computed bearing life is very close to that computed by the race lives only with the assumption of infinite ball life. However, it should be emphasized that this observation does not imply that for hybrid bearings the generalized LP model converges to the original LP model, which does not consider an independent ball life calculation. The empirical model constant in the original LP model, based on lives of AISI 52100 races only, is derived by correlating life predictions to experimental AISI 52100 bearing life data. The model constant in the generalized LP model, which is based on independent race and rolling element lives with arbitrary materials, is determined by correlating model predictions to experimental bearing life data with prescribed bearing materials. The empirical constant in the generalized model is therefore greatly different from the original LP constant, and it is independent of material properties. Although the two models provide identical results for AISI 52100 bearings, the results are different for other materials.

It should be noted that the above observations with regard to comparison of all-steel and hybrid bearings are specific to the present example of a 40-mm bore bearing operating at 10,000 rpm, where centrifugal forces are small relative to the applied loads. In high-speed turbine engine bearings, particularly at light loads, the centrifugal forces may result in a significant change in contact angles and loads, which affects life. Additional parametric studies are necessary to investigate the role of hybrid bearings in such applications.

Solutions for the GZ model are similar, except that at lower contact stresses the GZ lives are relatively higher due to a higher stress-life exponent.

Experimental data and model validation

The limited experimental data recently published by Trivedi, et al. *(14)* are perhaps the only experimental data currently available in the public domain for hybrid ball bearings. These data are used for initial experimental validation of the proposed enhancements of life models for hybrid ball bearings. The available experimental data are for the 40-mm bore ball bearing, described in Table 2. The bearing operates at a shaft speed of 10,000 rpm with an applied thrust load of 22,241 N (5,000 lbf). All test bearings are lubricated with the common MIL-PRF-23699 type lubricant and the bearing operating temperature is 400 K.

To establish a baseline, the first set of experimental data in Trivedi, et al. *(14)* is for an all-steel bearing with VIMVAR AISI M-50 races and balls, followed by a data set for hybrid bearings with silicon nitride balls and VIMVAR AISI M-50 races. In addition, hybrid bearings with silicon nitride balls and races made with M50NiL and the more recently developed case-hardened material Pyrowear 675 (P675) are considered in this experimental investigation. Although the experimental data are limited, they include both low-temperature-tempered (LTT) and high-temperature-tempered (HTT) P675 races against silicon nitride balls. Because the experimental data provide actual bearing life at prescribed operating conditions, whereas the life models presented above predict basic subsurface L_{10} fatigue life of the bearing with no life modification factors, it is essential to reduce the estimated experimental life with applicable life modification factors for a valid comparison with the analytical predictions. For this purpose, the applicable STLE life modification factors (Zaretsky *(16)*) are computed for each test condition. The experimentally determined L_{10} life is divided by these factors to estimate the basic experimental life.

The STLE life factors include life modification factors for materials, material processing, material hardness, and lubricant film thickness under pertinent operating conditions. For all test cases, the suggested materials factor is 2, and the materials processing factor is 6 for VIMVAR-type materials processing. Though the hardness values for M50, M50NiL,

Table 3a. Experimental bearing life data sets published by Trivedi et al *(14)*; 40-mm angular contact ball bearing operating with PRF-23699 lubricant, thrust load of 22,241 N (5,000 lbf), operating temperature of 400 K, and shaft speed of 10,000 rpm.

Data set	Ball/race materials	Race hardness (RC)	Contact stress (GPa)	Failure index
Set A	VIMVAR AISI M-50–VIMVAR AISI M-50	61	3.01	5/12
Set B	Silicon nitride–VIMVAR AISI M-50	61	3.37	9/20
Set C	Silicon nitride–M50NiL	61	3.50	8/16
Set D	Silicon nitride–P675 (LTT)	60	3.43	3/14
Set E	Silicon nitride–P675 (HTT)	66	3.43	2/12

Table 3b. Estimated basic L_{10} lives and associated statistical variation for the data sets as published by Trivedi, et al. *(14)*.

Data set	Estimated experimental L_{10} life (h)	90% Confidence band on L_{10} life (h)[a]	Applicable STLE life factor[b]	Estimated basic L_{10} life (h)	Expected variation in basic L_{10} life (h)
Set A	511	53–1,468	40	13	1–37
Set B	229	54–513	40	6	1–13
Set C	422	128–1,426	38	11	3–38
Set D	1,726	0–3,829	38	45	0–100
Set E	2,472	0–9,381	61	40	0–154

[a]Vlcek, et al. *(17)*.
[b]Zaretsky *(16)*.

and P675 LTT are similar, P675 HTT has been reported to have a significantly higher hardness. This results in a significantly higher hardness factor for the Pyrowear HTT material. Lubrication factors for all test cases are similar due to identical operating conditions; very small differences are related to the differences in computed lubricant film thickness due to small differences in elastic modulus of the race materials at the operating temperature. It should be noted that the life modification factors, although estimated from experimental bearing performance data, may have significant uncertainties. In addition to uncertainties in life modification factors, the L_{10} lives, as estimated by Weibull analysis, may be subject to significant uncertainties associated with statistical variation in experimental data and test sample size, as investigated by Vlcek, et al. *(17)*.

A summary of all five data sets published by Trivedi, et al. *(14)* is presented in Tables 3a and 3b. Table 3a lists the materials used, operating inner race contact stress, and observed failure indices, and Table 3b summarizes the experimental lives; expected variations, per statistical procedures developed by Vlcek, et al. *(17)*; and the derived basic lives using the applicable STLE life factors.

Note that the contact stresses listed in Table 3a are slightly lower than those presented by Trivedi, et al. *(14)*. The discrepancy is related to the value of elastic modulus at operating temperature. The current effort includes a variation in elastic modulus with operating temperature *(18)*, whereas Trivedi, et al. *(14)* disregarded this variation and used the elastic modulus at room temperature. This is confirmed by performing contact stress computation at both temperatures.

For the purpose of model validation, the estimated experimental L_{10} lives are divided by applicable STLE life factors (Zaretsky *(16)*) to derive the estimated basic L_{10} lives. For each of the five data sets, these derived basic L_{10} lives and associated statistical variations, as derived from experimental L_{10} lives and applicable STLE life factors, are summarized in Table 3b. Because the analytical model is based on the well-established Weibull slope of 1.111, determined from analysis of a large amount of experimental bearing life data by Lundberg and Palmgren *(1, 2)*, the WeiBayes constraint is used to estimate the L_{10} life with a constraint Weibull slope of 1.111.

Weibull plots of the experimental data set A with all-steel VIMVAR AISI M-50 bearings and set B with VIMVAR AISI M-50 races and silicon nitride balls are shown respectively in Figs. 4 and 5. The dashed lines in Figs. 4 and 5 represent the expected life with the WeiBayes constraint. The expected variations (90% confidence limits) in the estimated L_{10} lives, per relations presented by Vlcek, et al. *(17)*, are also documented in Figs. 4 and 5.

Note that the L_{10} lives with the WeiBayes constraint are quite close to those determined by the Weibull solutions obtained by a least-squared fit to the experimental data. At the prescribed thrust load of 22,241 N, the L_{10} life of the hybrid bearing is notably lower that for the all-steel bearing.

Experimental basic L_{10} lives, derived from the data shown in Figs. 4 and 5, after applying the applicable STLE life modification factors (Zaretsky *(16)*) as documented in Table 3b, are compared with life predictions obtained with the enhanced LP and GZ life models in Fig. 6. The expected statistical variation in the estimated basic experimental lives is also displayed in Fig. 6.

Clearly, the life predictions by both the enhanced LP and GZ models are reasonably close to the experimental L_{10} life estimated from the experimental data. In addition, at a prescribed operating load, the life predictions provided by both models demonstrate that the hybrid bearings have a lower life in comparison to the all-steel bearings, as seen experimentally. However, in view of limited experimental data, uncertainties in the computation of life modification factors, and uncertainties in operating variables, such as temperature, the relatively small differences between model predictions and experimental observations are statistically insignificant.

In addition to VIMVAR AISI M-50, Trivedi, et al. *(14)* provided some experimental life data for hybrid bearings with case-hardened M50NIL and Pyrowear 675 (P675) races and silicon nitride balls. In case of P675, both the LTT and HTT versions of the material are considered. For the LTT version of P675 material, the material is tempered at 583 K (600 °F) to produce a hot hardness of about 61 RC at a

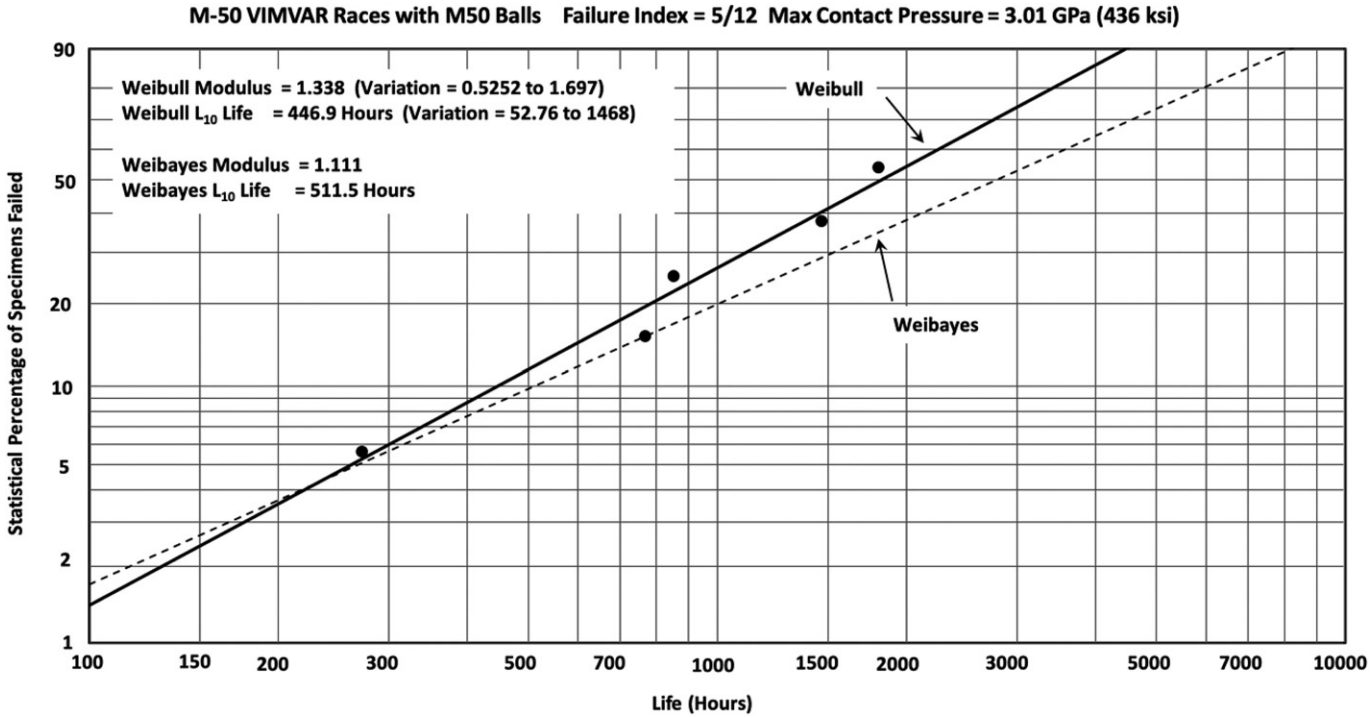

Figure 4. Weibull plot of experimental data obtained with the 40-mm ball bearing, with VIMVAR AISI M-50 races and balls (data set A in Table 3a), operating at 10,000 with a thrust load of 22,241 N (5,000 lbf; Trivedi, et al. *(14)*).

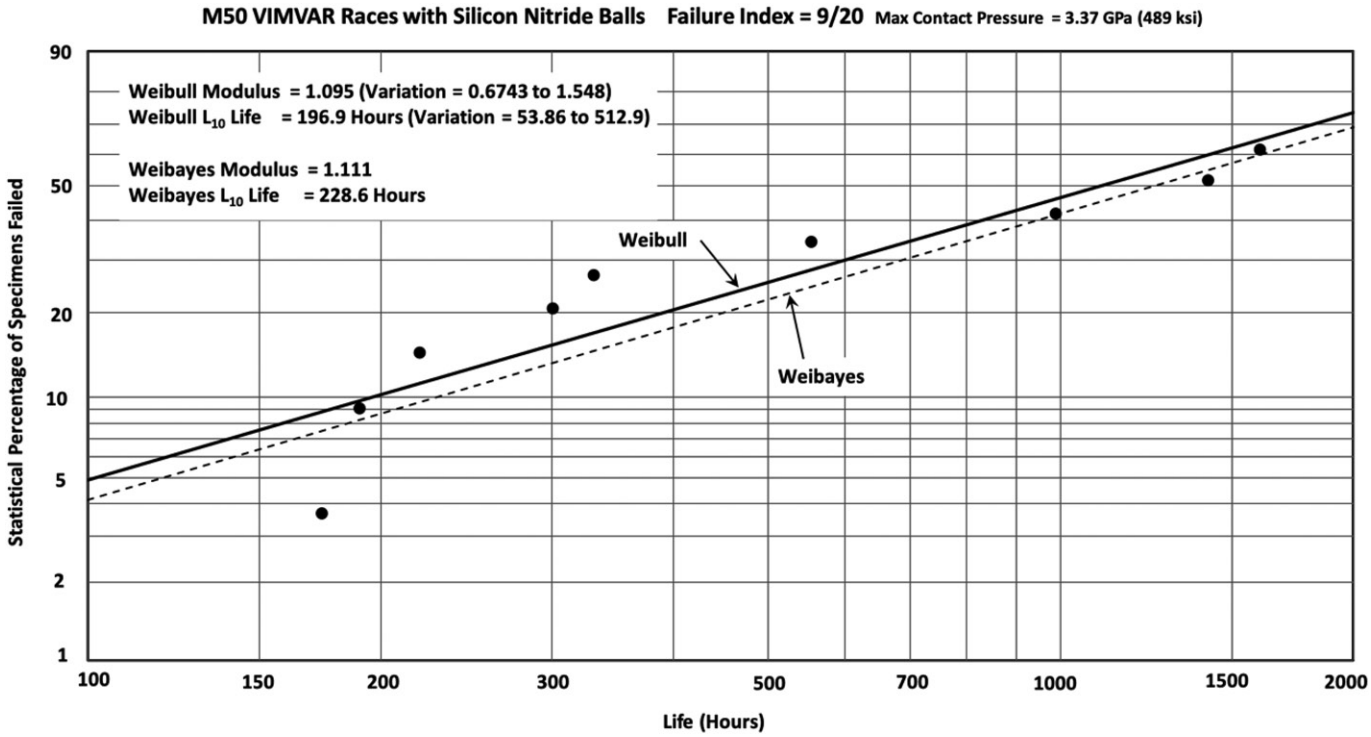

Figure 5. Weibull analysis for experimental life data obtained with the 40-mm hybrid bearing, with VIMVAR AISI M-50 races and silicon nitride balls (data set B in Table 3b), operating at 10,000 rpm with a thrust load of 22,241 N (5,000 lbf; Trivedi, et al. *(14)*).

temperature of 400 K, which is comparable to the hot hardness of M50NiL. A significantly higher hot hardness is produced in the HTT version of P675, where the material is tempered at 769 K (925 °F) to produce a higher hot hardness of about 65 RC at a temperature of 400 K as reported by Trivedi, et al. *(14)*. In addition, Klecka, et al. *(19)* provided similar hardness measurements for these materials along with the variation of elastic modulus with case depth. Whereas the failure index of M50NiL bearings is 8/16, it is only 3/14 and 2/12 respectively for the LTT and HTT versions of P675. Although these limited numbers of failures yield a rather large range of statistical variation in estimated

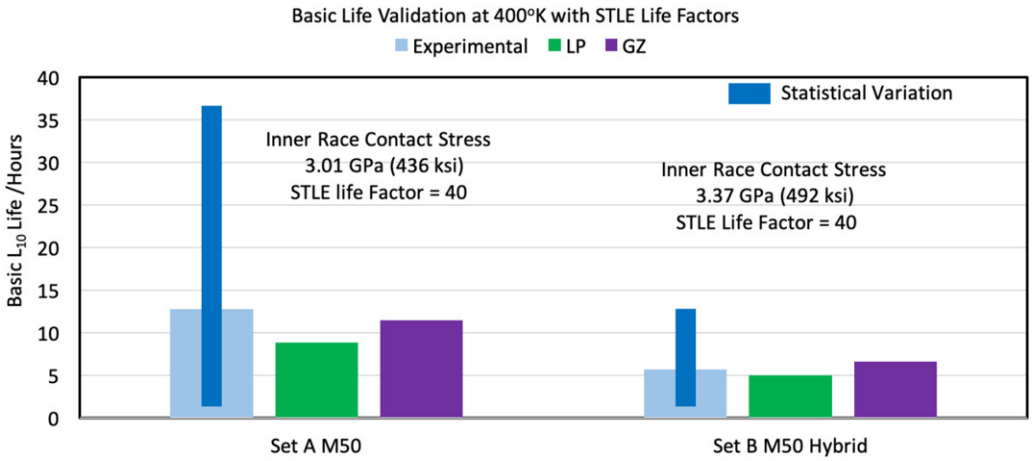

Figure 6. Validation of life predictions obtained from the enhanced LP and GZ life models against experimental life data, as published by Trivedi, et al. *(14)*, for both the all-steel and hybrid ball bearings.

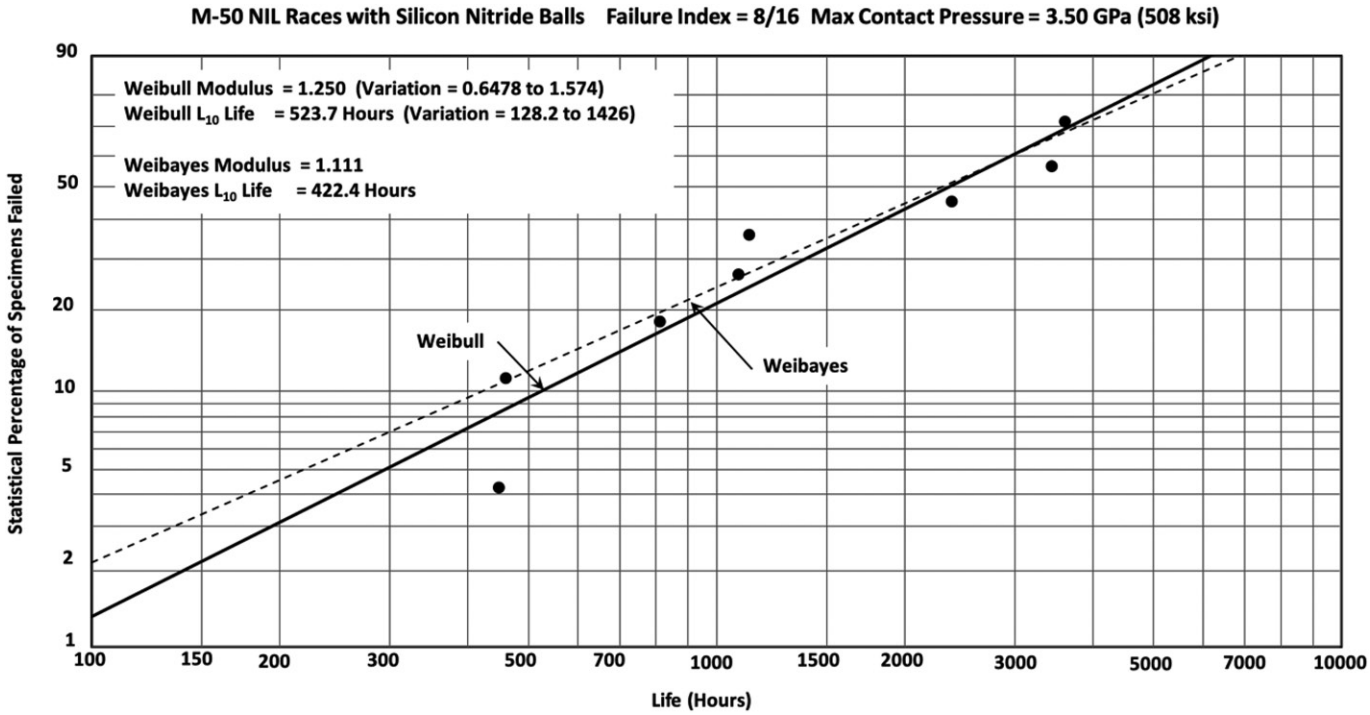

Figure 7. Life data for 40-mm hybrid ball bearing with M50NiL races and silicon nitride balls (data set C in Table 3a) operating at 400 K with a thrust load of 22,241 N (5,000 lbf) and shaft rpm of 10,000 rpm (Trivedi, et al. *(14)*).

L_{10} life, P675 HTT does seem to provide a notably higher life when compared to the LTT version of the material. Such an observation supports the STLE life modification factor for hardness (Zaretsky *(16)*).

Case-carburized materials, such as M50NiL and P675, contain significant compressive residual stress buildup as a part of the manufacturing process. Trivedi, et al. *(14)* have reported compressive residual stresses in the range of 200 to 300 MPa for both M50NiL and P675. In addition, Rosado, et al. *(20)* reported residual stresses in the range of 100 to 300 MPa for M50NiL.

For realistic modeling of life in the case of hybrid ball bearings with case-hardened materials, it is essential that in addition to modeling the fatigue behavior of silicon nitride, as done in the current investigation, both the effect of compressive residual stress and elastic modulus variation with case depth be considered in the life models. This has been recently done by Gupta *(21)*, and the resulting model enhancements are included in the enhanced version of ADORE used in the present investigation. Though the variation in elastic modulus with depth is modeled in terms of an effective elastic modulus, a failure stress modification procedure is implemented to model the effect of both residual and hoop stresses in bearing races. In addition, elastic modulus variation with operating temperature, as available in the open literature *(18)*, has also been implemented. In fact, ADORE implements thermal effects at two levels: first, all material properties are temperature dependent and,

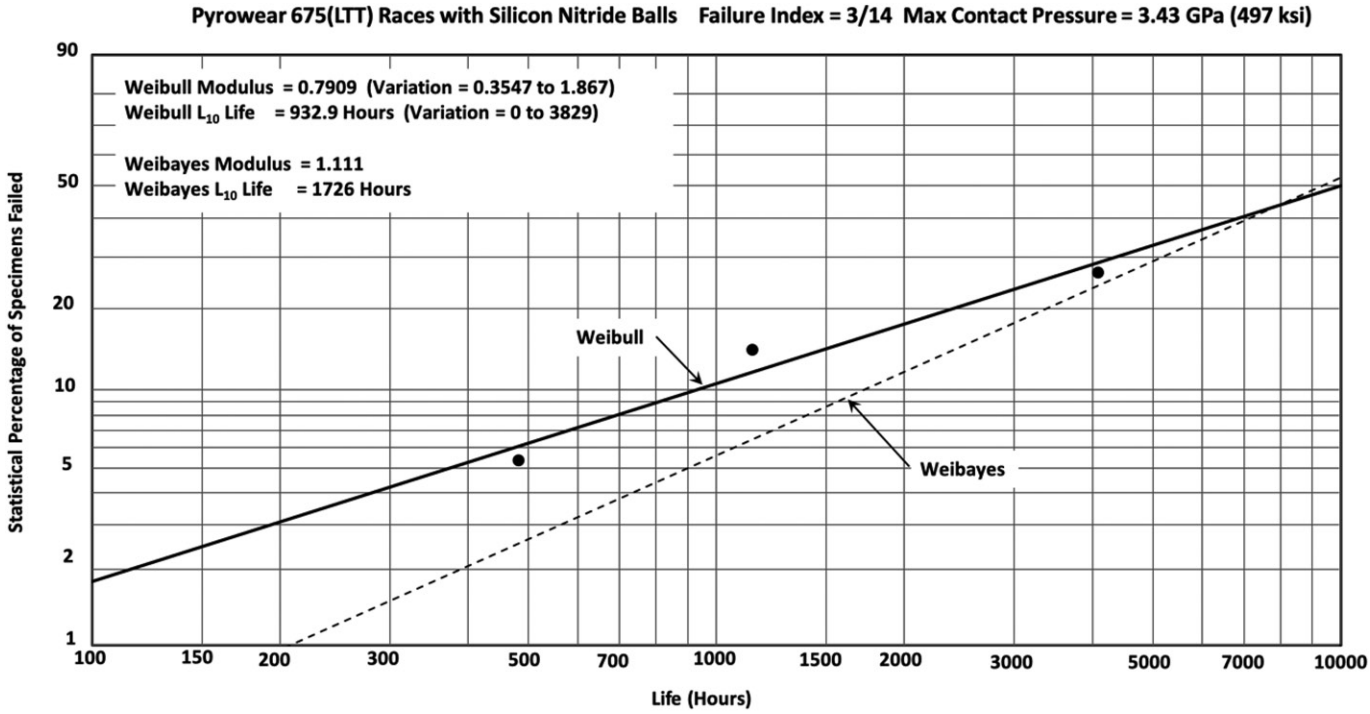

Figure 8. Experimental fatigue life data for the 40-mm angular contact hybrid ball bearing with P675 (LTT) races and silicon nitride balls (data set D in Table 3a) operating at 400 K with a thrust load of 22,241 N (5,000 lbf) and a race speed of 10,000 rpm (Trivedi, et al. *(14)*).

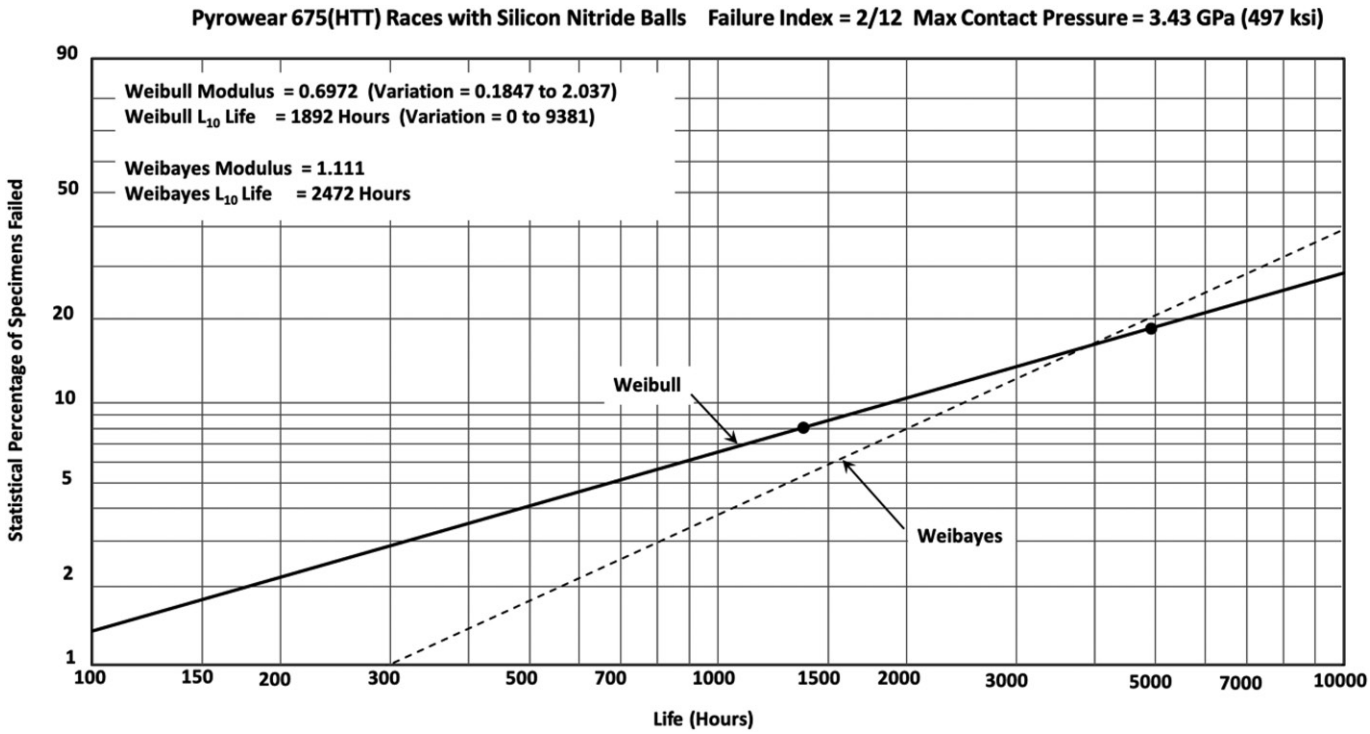

Figure 9. Experimental fatigue life data for the 40-mm angular contact hybrid ball bearing with P675 (HTT) races and silicon nitride balls (data set E in Table 3a) operating at 400 K with a thrust load of 22,241 N (5,000 lbf) and a race speed of 10,000 rpm (Trivedi, et al. *(14)*).

secondly, bearing geometry is altered as a function of temperature to allow for thermal distortion. The effect of initial shrink fits and centrifugal expansion of races at the operating speed is also included while modeling the operating race geometry at prescribed temperature.

Figures 7, 8, and 9 respectively contain the data sets for hybrid bearings with silicon nitride balls and races made out of M50NIL and the LTT and HTT versions of P675.

Experimental validation of basic L_{10} life predictions for hybrid bearings with case-hardened race materials is

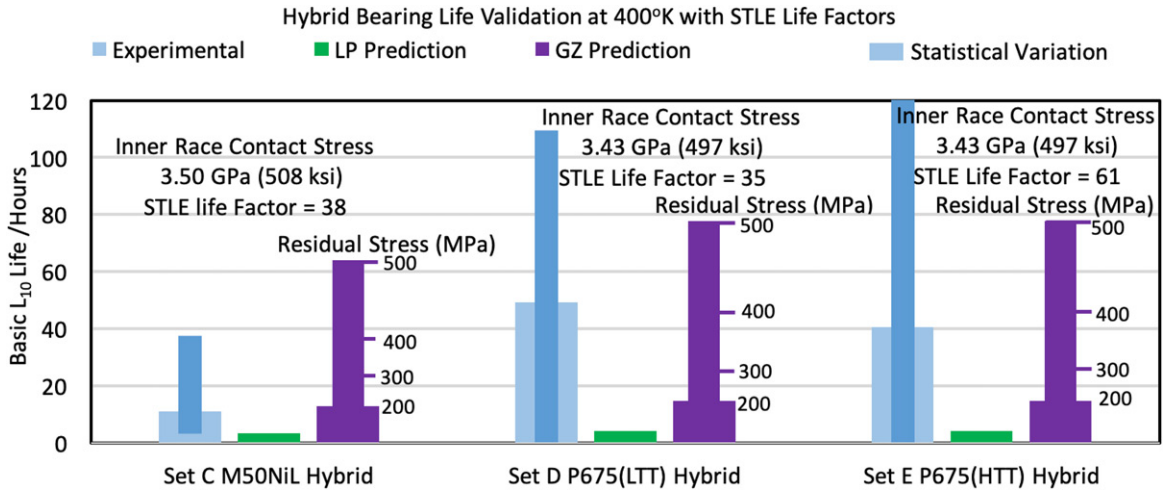

Figure 10. Validation of basic L_{10} life predictions against experimental data for hybrid ball bearings, with case-hardened race materials, operating at 10,000 rpm with a thrust load of 22,241 N (5,000 lbf) at an operating temperature of 400 K, as presented by Trivedi, et al. *(14)*.

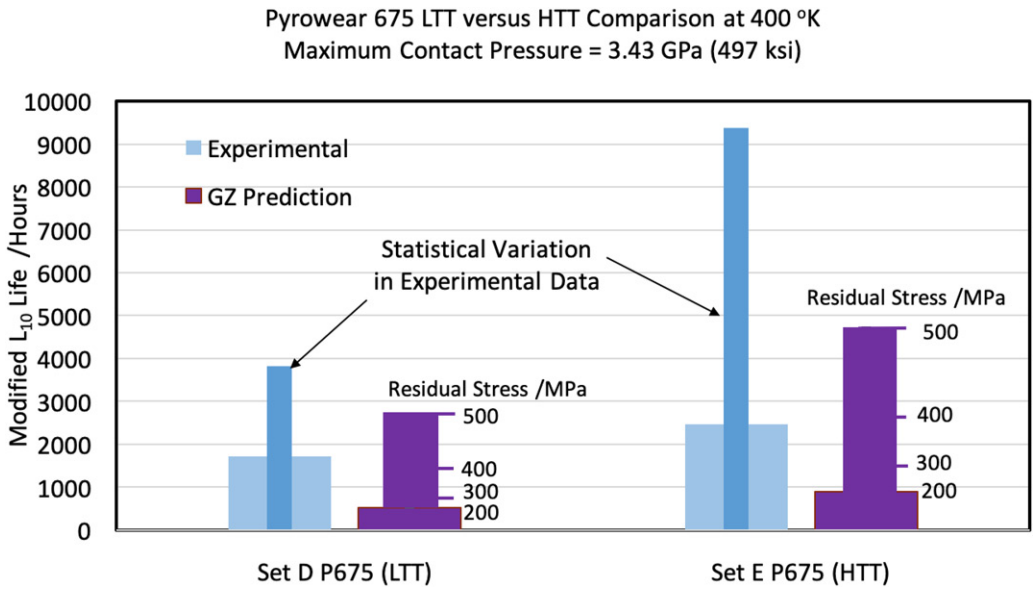

Figure 11. Comparison of experimental (as published by Trivedi, et al. *(14)*) and predicted lives for 40-mm hybrid ball bearing operating at 10,000 rpm with a thrust load of 22,241 N (5,000 lbf) and an operating temperature of 400 K, with silicon nitride balls and races made out of the LTT and HTT versions of P675.

presented in Fig. 10. In support of these validations, it is essential to clarify the following:

1. Because the LP model is based on maximum subsurface orthogonal shear stress, which is unaffected by residual stresses, the predicted lower LP life with case-hardened materials is not realistic. Thus, until the LP model is further refined, only the GZ model, based on maximum subsurface shear stress should be considered for life modeling with case-hardened materials.
2. The predicted GZ lives in Fig. 10 are shown as a function of the level of compressive residual stress. The main broad bar in the figure corresponds to a base compressive residual stress of 200 MPa (29 ksi), as reported by Trivedi, et al. *(14)*, and the added thinner bar shows increased life as a function of increasing level of compressive residual stress.
3. The notably increased range of statistical variation in experimental life with the Pyrowear material corresponds to greatly reduced failure indices: 3/14 for the LTT and 2/12 for HTT versions of P675.
4. Model predictions of basic lives are identical for P675 LTT and HTT materials. This is due to the fact that the input elastic properties for both these materials are identical.
5. Though actual experimental life with P675 HTT is higher in comparison to P675 LTT, the basic life shown for the HTT material is lower than that for the LTT material in Fig. 10. This is due to the fact the STLE life modification factor resulting from a notably higher hardness of the HTT material is significantly higher for P675 HTT in comparison to P675 LTT; the basic life plotted in Fig. 10 is actual life divided by the applicable life modification factor.

Perhaps a better comparison of both the experimental observations and model predictions for the two versions of P675 may be presented in terms of actual observed life and the predicted modified life as determined by application of life modification factors on the computed basic subsurface life. This is done in Fig. 11. Clearly, both the experimental and predicted lives for HTT Pyrowear are higher than those for the LTT version of the material.

In view of the limited experimental data, the current investigation should only be regarded as initial validations for the life models developed herein. However, the generalities in terms of modifications of all empirical constants and life exponents the generalized models greatly facilitate continued enhancement as additional experimental data become available.

Summary

Based upon the available experimental data on the rolling contact fatigue life of silicon nitride balls, the rolling element life model is enhanced in the generalized fatigue life models recently developed by Gupta and Zaretsky *(7)*. Enhancement of the empirical constant and stress-life exponent in the ball life equation is based on the following two experimental findings with regard to fatigue behavior of silicon nitride:

1. The stress-life exponent for a silicon nitride ball in rolling contact is 16.
2. LP lives of silicon nitride and AISI 52100 steel balls are equal at a contact stress of 5.516 GPa (800 ksi).

The enhanced ball life equation is combined with the generalized life equations for the races to develop a life prediction model for a hybrid ball bearing. Initial experimental validations of model predictions are presented against the available limited full-scale hybrid ball bearing test data presented by Trivedi, et al. *(14)* for a 40-mm angular contact ball bearings with silicon nitride balls and the races made out of AISI VIMVAR AISI M-50 steel and case-hardened materials M50NiL and Pyrowear 675 (P675). Both the LTT and HTT versions of P675 are considered. Key findings from the model enhancement and validation tasks are as follows:

1. For hybrid bearings, the calculated lives of silicon nitride balls are significantly greater than those of the steel inner and outer races. Therefore, by assuming infinite silicon nitride ball life, the bearing life can be reasonably well calculated by race lives only in the life models recently generalized by Gupta and Zaretsky *(7)*.
2. For case-hardened materials, such M50NiL and PyroWear 675 (P675), the compressive residual stresses have a dominant effect on bearing life. Although the current LP model does not permit direct modeling of these stresses, the GZ model implements an appropriate failure stress modification to model the impact of residual stresses on bearing life.
3. Due to significantly higher hot hardness of the HTT version of P675 in comparison to the LTT material, which has a hot hardness comparable to AISI M50 and M50NiL, the hybrid bearing with P765 (HTT) races and silicon nitride balls provides higher life in comparison to that obtained with P675 (LTT) races and silicon nitride balls. This provides added validation to the commonly used STLE hardness life factor.
4. Life predictions obtained with the enhanced model for hybrid bearings are in good agreement with the experimental findings.

Acknowledgements

Technical support provided by Hitesh Trivedi of UES Inc. in the compilation and interpretation of experimental data is gratefully acknowledged.

Funding

Work reported in this article was carried out under a U.S. Air Force Small Business Innovation Research (SBIR) Phase II (Contract #FA8650-15-C-2534) contract awarded to PKG Inc. The Air Force Technical Contract Monitor was Jeremy Nickell.

References

(1) Lundberg, G. and Palmgren, A. (1947), "Dynamic Capacity of Rolling Bearings," *Acta Polytechnica Mechanical Engineering Series*, **1**(3), pp 7.

(2) Lundberg, G. and Palmgren, A. (1952), "Dynamic Capacity of Roller Bearings," *Acta Polytechnica Mechanical Engineering Series*, **2**(4), pp 96.

(3) Weibull, W. (1939), "A Statistical Theory of the Strength of Materials," *Inginiors Vetenskaps Adademien*, **151**.

(4) Zaretsky, E. V. (1989), "Ceramic Bearings for Use in Gas Turbine Engines," *Journal of Engineering for Gas Turbines and Power*, **111**(1), pp 146–157.

(5) Baumgartner, H. R. and Cowley, P. E. (1975), "Silicon Nitride in Rolling Contact Bearings," **NTIS AD-A015990**.

(6) Baumgartner, H. R., Calvert, G. S., and Cowley, P. E. (1976), "Ceramic Materials in Rolling Contact Bearings," **NTIS AD-A031560**.

(7) Gupta, P. K. and Zaretsky, E. V. (2018), "New Stress-Based Fatigue Life Models for Ball and Roller Bearings," *Tribology Transactions*, **61**(2), pp 304–324.

(8) Zaretsky, E. V. (1987), "Fatigue Criterion to System Design, Life and Reliability," *AIAA Journal of Propulsion and Power*, **107**(3), pp 76–83.

(9) Yu, W. K. and Harris, T. A. (2001), "A New Stress-Based Fatigue Life Model for Ball Bearings," *Tribology Transactions*, **44**(1), pp 11–18.

(10) Ioannides, E. and Harris, T. A. (1985), "New Fatigue Life Model for Rolling Bearings," *Journal of Lubrication Technology*, **107**(3), pp 367–378.

(11) Parker, R. J. and Zaretsky, E. V. (1975), "Fatigue Life of High-Speed Ball Bearings with Silicon Nitride Balls," *Journal of Lubrication Technology*, **97**(3), pp 350–357.

(12) Parker, R. J. and Zaretsky, E. V. (1972), "Reevaluation of the Stress-Life Relation in Rolling-Element Bearings," **NASA TN D-6745**.

(13) Parker, R. J. and Zaretsky, E. V. (1972), "Rolling-Element Fatigue Lives of Through-Hardened Bearing Materials," *Journal of Lubrication Technology*, **94**(2), pp 165–173.

(14) Trivedi, H. K., Rosado, L., Gerandi, D. T., Givan, G. D., and McCoy, B. (2017), "Fatigue Life Performance of Hybrid Angular Contact P675 Bearings," *Bearing and Steel Technologies: Vol. 11. Progress in Steel Technologies and Bearing Steel Quality*, Beswick, J. M. (Ed.), pp 275–299, ASTM International: West Conshohocken, PA.

(15) Gupta, P. K. (1984), *Advanced Dynamics of Rolling Elements*, Springer-Verlag: New York.

(16) Zaretsky, E. V. (1992), *STLE Life Factors for Rolling Bearings*, STLE: Park Ridge, IL.

(17) Vlcek, B. L., Hendricks, R. C., and Zaretsky, E. V. (2003), "Determination of Rolling-Element Fatigue from Computer Generated Bearing Tests," *Tribology Transactions*, **46**(4), pp 479–493.

(18) "Material Data Sheet, Latrobe Lescalloy, M-50 VIMVAR." Available at: http://www.matweb.com (accessed June 30, 2017)

(19) Klecka, M. A., Subhash, G., and Arakere, N. K. (2013), "Micro-Structure Property Relationships in M50NIL and P675 Case Hardened Bearing Steels," *Tribology Transactions*, **56**(6), pp 1046–1059.

(20) Rosado, L., Forster, N. H., Thompson, K. L., and Cooke, J. W. (2010), "Rolling Contact Life and Spall Propagation of AISI M50, M50NiL and AISI 52100, Part I: Experimental Results," *Tribology Transactions*, **53**(1), pp 29–41.

(21) Gupta, P. K. (2019), "Failure Stress Modification in Fatigue Life Models for Rolling Bearings," *Proceedings of the Institution of Mechanical Engineers - Part J: Journal of Engineering Tribology*, **233**(9), pp 1327–1344.